27/28th International Conference
ENGINEERING MECHANICS 2022
Milovy, Czech Republic, May 9 –12, 2022
Paper **#15**, pp. 389–392, doi: 10.21495/51-2-389

NUMERICAL AND EXPERIMENTAL AERODYNAMIC INVESTIGATION OF SMALL-SIZED IMPULSE-TYPE TURBINE STAGE

Straka P.*, **Němec M.****

Abstract: *Numerical and experimental investigation of flow in a small-sized axial turbine stage of impulse type was carried out in order to determine the aerodynamic and energy parameters. Special attention was paid to over-loaded regimes with negative value of the thermodynamic reaction. This study pointed on a strong effect of a leakage flow from a hub labyrinth seal on the stage efficiency. Numerical simulation allowed to study a development of a secondary flow structures in peripheral parts of a blade span. In this paper there are compared results of numerical simulations and experimental investigation.*

Keywords: Axial turbine stage, Impulse-type stage, Secondary flow, Leakage flow, Efficiency.

1. Introduction

The contribution deals with numerical and experimental investigation of aerodynamic and energy properties of the small-sized impulse-type axial turbine stage. Figure 1 shows a scheme of such turbine stage installed in a experimental test facility. The blade geometry of this turbine stage corresponds with the small-sized turbines in production of the PBS ENERGO a.s. company. This type of turbine stage is characterised with relatively small value of the span to chord ratio. In this case, the ratio is approximately 0.97 for the stator blades and 1.19 for the rotor blades. These values indicates strong influence of the secondary flows in the peripheral parts of the blades span on the aerodynamic and energy properties.

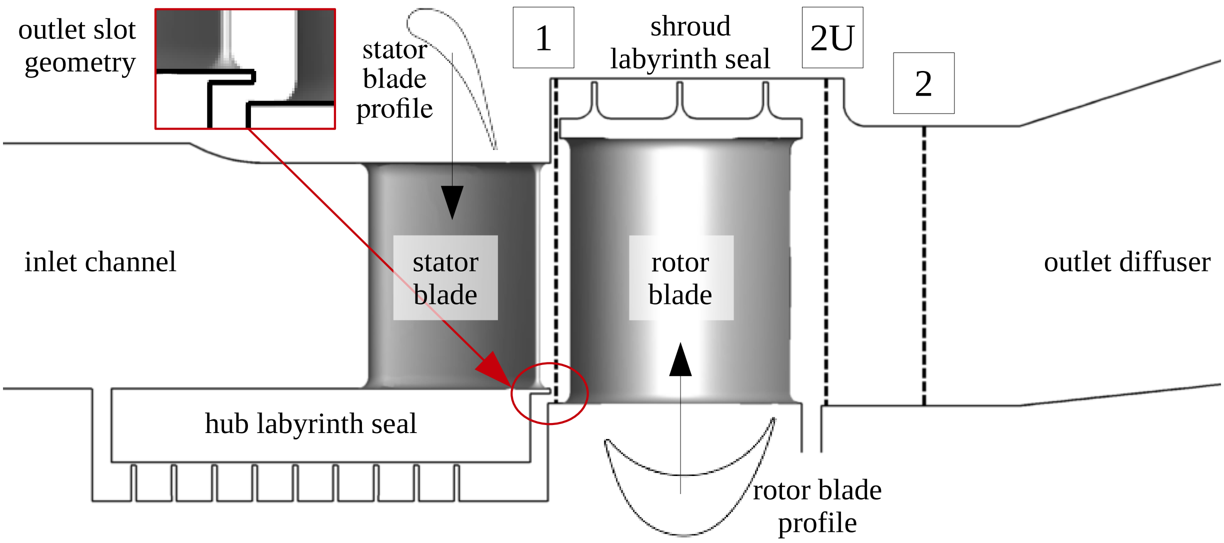

Fig. 1: Scheme of the small-sized impulse-type axial turbine stage.

Flow path of investigated stage is consisted of the inlet channel, the stator blade, the hub labyrinth seal, the rotor blade, the shroud labyrinth seal and the outlet diffuser. The stator and rotor wheels are composed of 51 and 92 prismatic blades respectively. The blades profiles are also shown in Fig. 1.

* Ing. Petr Straka, Ph.D.: Czech Aerospace Research Centre, Beranových 130; 199 05, Prague; CZ, straka@vzlu.cz
** Ing. Martin Němec, Ph.D.: Czech Aerospace Research Centre, Beranových 130; 199 05, Prague; CZ, nemec@vzlu.cz

Two geometry configurations were studied: a) fully opened hub labyrinth seal - marked as V1, b) closed hub labyrinth seal (zero radial gap above the seal fins) - marked as V2. In configuration V2 the geometry of the outlet slot from the hub labyrinth seal (shown in Fig. 1) is remained.

The experimental investigation was carried out in a high speed laboratory of the VZLU, a.s. The test rig is a part of the high-speed closed-loop wind tunnel which allows independent setting of the Mach and the Reynolds number. Tested turbine is loaded by hydraulic dynamometer Froude Hofmann F249-Race GT. Flange torque meter HBM T10FS is used for the connection of turbine's and dynamometer's shafts in order to in- crease the accuracy of the torque measurement. More details can be found in (Nemec, 2021).

Calculations of flow were performed using the in-house numerical software developed in laboratory of high speed aerodynamics of the VZLU, a.s. This software is based on solution of RANS equations closed with two-equations turbulence model using the finite volumes discretization method. In this work, the interaction between the stator and rotor domains is of the *mixing plane* type. For more details see (Straka, 2012) and (Straka, 2016/a). The nonlinear explicit algebraic model of the Reynolds stress is used in this work according to Rumsay and Gatski (2001).

Operation regimes are defined with expansion ratio $p_{T0}/p_{S2} = 1.714$ and velocity ratio in range $0.25 \leq u/c \leq 0.6$, where p_{T0} is the inlet total pressure, p_{S2} is the outlet static pressure, u is the circumferential velocity at the middle diameter and c is the isentropic outlet velocity. The Reynolds number based on the isentropic outlet velocity and axial blade chord is approx 4×10^5. The flowing medium is dry air.

2. Results

In figure 2a) there is shown comparison of the total-total and total-static efficiency in dependence on the velocity ratio. The total-total and total-static efficiency is defined as $\eta_{TT/TS} = (T_{T0} - T_T)/(T_{T0} - T_{TT/TS\,is})$, where T_{T0} is the total inlet temperature, T_T is the local total temperature, $T_{TT/TS\,is}$ is the local isentropic total/static (respectively) temperature. The dependence of the thermodynamic reaction on the velocity ratio is shown in figure 2b). The thermodynamic reaction is defined as $\rho = (T_{S1\,is} - T_{S2U\,is})/(T_{T0} - T_{S2U\,is})$, where $T_{S1\,is}$ and $T_{S2U\,is}$ are the static isentropic temperatures in planes 1 and 2U respectively. The evaluation planes 1, 2U and 2 are indicated in Fig. 1.

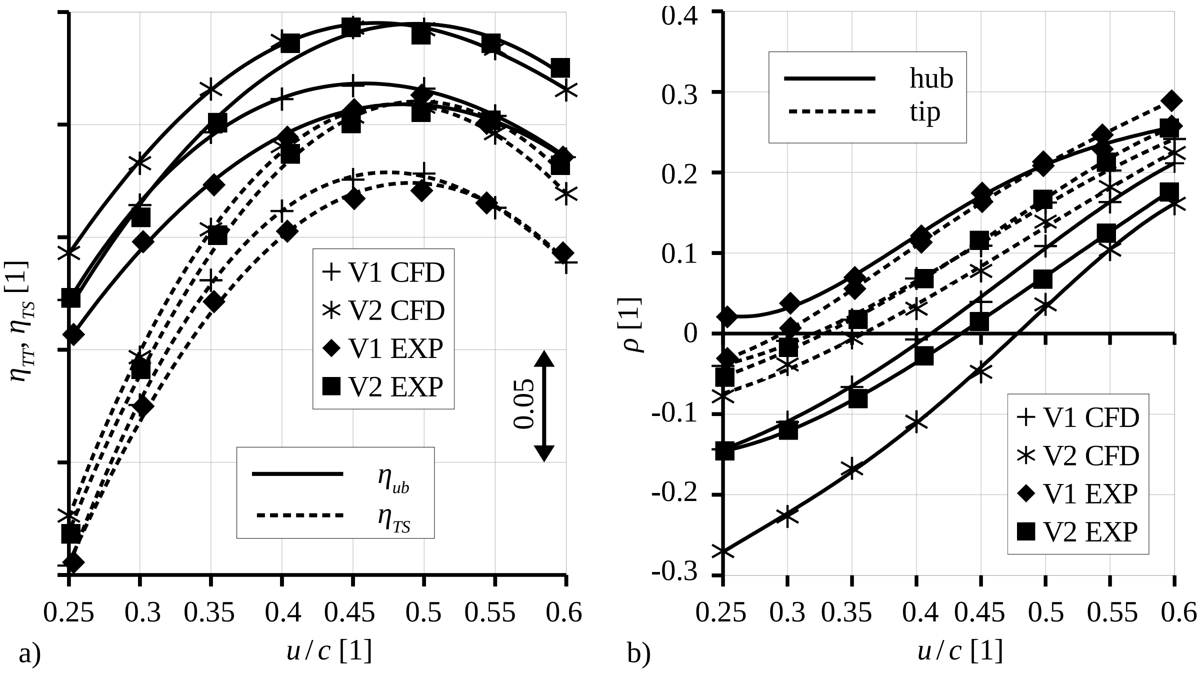

Fig. 2: The efficiency dependence on u/c (a); the thermodynamic reaction dependence on u/c (b).

In figure 2b) there are plotted curves of the thermodynamic reaction for hub and tip diameters. It is evident that the thermodynamic reaction is negative at the hub diameter up to velocity ratio 0.45 (which is optimal regime with maximum efficiency) whereas at the tip diameter the thermodynamic reaction remain negative for overloaded regimes only (velocity ratio under value 0.35). The radial distribution of the thermodynamic reaction is shown in figure 3b) for the most overloaded and the optimal regimes. The negative value of the thermodynamic reaction indicates that the rotor blades work in compressor regime. It means that the pressure behind the rotor blades is higher than behind the stator blades. By other words, the flow in the rotor wheel takes place under conditions of an adverse pressure gradient with impact on the boundary layer thickness development. Another consequence of the negative thermodynamic reaction is the opposite direction of the axial force on the rotor disk.

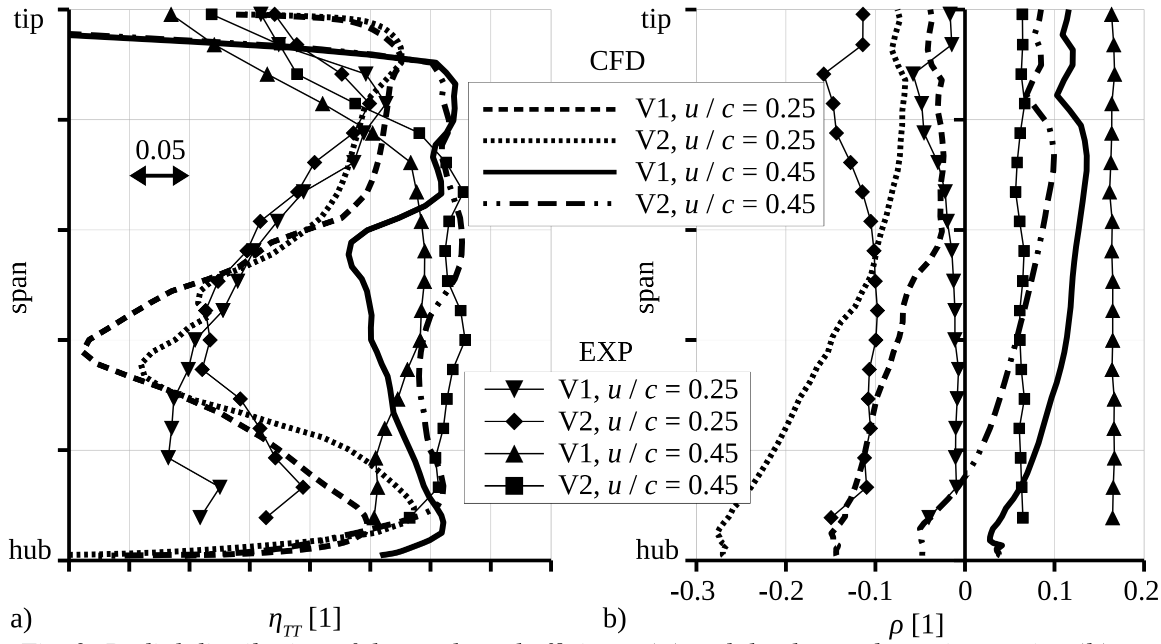

Fig. 3: Radial distribution of the total-total efficiency (a) and the thermodynamic reaction (b).

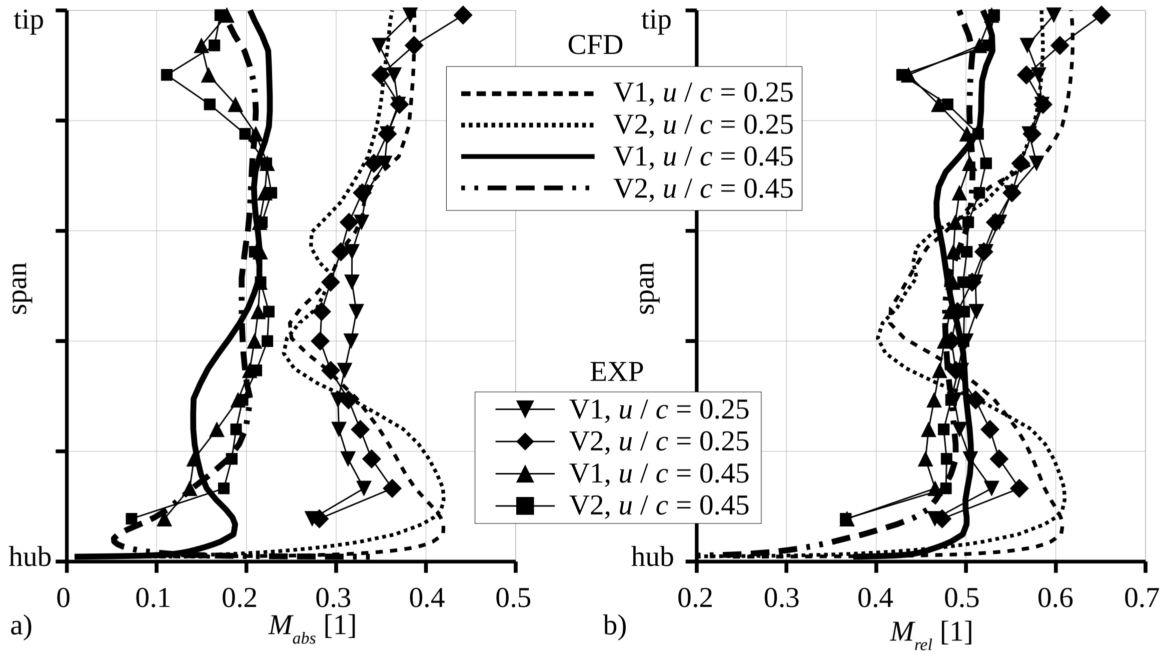

Fig. 4: Radial distribution of the absolute (a) and relative (b) Mach number.

Figure 4 shows comparison of the radial distributions of the absolute and relative Mach number in plane 2 for the most overloaded and the optimal regimes. Comparison of numerical and experimental results in figures 2 – 4 shows relatively good agreement in prediction of the total-static efficiency η_{TS} dependence on the velocity ratio. There are some differences in determining of the total-total efficiency η_{TT}. The reason can be seen in used physical model of the stationary interaction of the stator and rotor blades with the *mixing plane* interface. This approach is effective in terms of the computing effort, but on the other hand it doesn't allow to predict an unsteady behaviour of the secondary flow structures. The largest differences between numerical and experimental data can be found in the radial distribution of the thermodynamic reaction in figure 3b). Contrary to the numerical results the experimental data shows almost constant radial distribution of the thermodynamic reaction. It means that in conditions of aerodynamic experiment there is constant radial distribution of the static pressure in front as well as behind the rotor blades.

In figure 5 there are shown the stream lines on the suction side of the rotor blade for optimal and the most overloaded regime. Contours displayed on the blade surface represents distribution of the thermodynamic reaction (light color for positive values, dark color for negative values). For the optimal regime $u/c = 0.45$ we can observe a difference in size of the area affected by the secondary flow in the hub region. This is due to the leakage flow from the hub labyrinth seal in variant V1. The area affected by the secondary flow in the tip region is approximately the same for both variants V1 and V2. It is obvious that in the case of the most loaded mode $u/c = 0.25$ entire blade span is affected by the secondary flows.

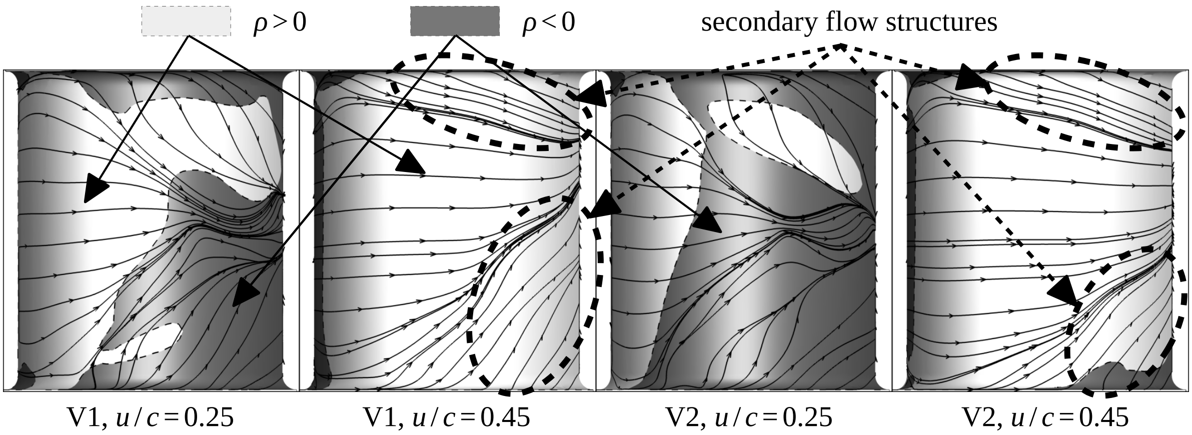

Fig. 5: The streamlines and the thermodynamic reaction distribution on the suction side of the rotor blade.

3. Conclusions

The paper describes numerical and experimental research of flow in the small-sized impuls-type axial turbine stage. From the numerical and experimental results, the dependence of the stage efficiency on the velocity ratio was compiled for two configurations of the hub labyrinth seal. It turns out that the leakage flow from the hub labyrinth seal significantly reduces the value of the stage efficiency. Some differences between numerical and experimental results were found. In particular, this concerns the radial distribution of the flow parameters behind the rotor blades. Therefore, future work will be focused on a more detailed analysis of the flow parameters radial distribution in front of and behind the rotor blades for a better understanding of the dissipative structures development. An experiment is being prepared with a detailed measurement of the radial distribution of the flow parameters in the axial gap between the stator and rotor blades. At the same time, the simulation of non-stationary interaction of stator and rotor blades will be performed using the method developed for simulations of high-swirl flow according to (Kok et al, 2004) and applied, e.g., in works (Straka, 2016/b) and (Straka, 2020).

Acknowledgments

This result was realised with the support of the Technology Agency of the Czech Republic within the THETA program, project No. TK02020081.

References

Kok, J.C., Dol, H.S., Oskam, B., and H. van der Ven (2004), Extra-large eddy simulation of massively separated flows. *AIAA paper*, 2004-264.

Nemec, M., and Jelinek, T. (2021), Adaptable test rig for two-stage axial turbine. *MATEC Web of Conferences*, Vol 345, Article Number 00022.

Rumsay, C.L., and Gatski, T.B. (2001), Recent turbulence model advances applied to multi-element airfoil computations. *Jour. Of Aircraft*, Vol. 83, pp. 904-910.

Straka, P. (2012), Simulation of a 3D unsteady flow in an axial turbine stage. *EPJ Web of conferences*, Vol 25, paper ID 01090.

Straka, P. (2016/a), Modelling of unsteady secondary vortices generated behind the radial gap of the axial turbine blade wheel. *Proc. ECCOMAS Congress 2016*, Crete.

Straka, P. (2016/b), Hybrid RANS/LES modelling of secondary flow in axial turbine stage. In: Zolotarev, I., and Radolf, V., eds., *Engineering Mechanics 2016.* IT of the CAS, Prague, pp. 555–558.

Straka, P., and Pelant, J. (2020), Prediction of the overloaded axial turbine stage efficiency using the hybrid RANS/LES turbulence model. In: Fuis V., ed., *Engineering Mechanics 2020.* VUT Brno, pp. 464–467.